Trafficking of Crumbs3 during cytokinesis is crucial for lumen formation

Molecular Biology of the Cell
Vol. 20, 4652–4663, November 15, 2009

Trafficking of Crumbs3 during Cytokinesis Is Crucial for Lumen Formation

Marc A. Schlüter,*† Catherine S. Pfarr,*† Jay Pieczynski,‡ Eileen L. Whiteman,* Toby W. Hurd,* Shuling Fan,* Chia-Jen Liu,* and Ben Margolis*‡

*Departments of Internal Medicine and ‡Biological Chemistry, University of Michigan Medical School, Ann Arbor, MI 48109; and †Medizinische Klinik D, Universitätsklinikum Münster, D-48149 Münster, Germany

Submitted February 17, 2009; Revised August 27, 2009; Accepted September 16, 2009
Monitoring Editor: David G. Drubin

Although lumen generation has been extensively studied through so-called cyst-formation assays in Madin-Darby canine kidney (MDCK) cells, an underlying mechanism that leads to the initial appearance of a solitary lumen remains elusive. Lumen formation is thought to take place at early stages in aggregates containing only a few cells. Evolutionarily conserved polarity protein complexes, namely the Crumbs, Par, and Scribble complexes, establish apicobasal polarity in epithelial cells, and interference with their function impairs the regulated formation of solitary epithelial lumina. Here, we demonstrate that MDCK cells form solitary lumina during their first cell division. Before mitosis, Crumbs3a becomes internalized and concentrated in Rab11-positive recycling endosomes. These compartments become partitioned in both daughter cells and are delivered to the site of cytokinesis, thus forming the first apical membrane, which will eventually form a lumen. Endosome trafficking in this context appears to depend on the mitotic spindle apparatus and midzone microtubules. Furthermore, we show that this early lumen formation is regulated by the apical polarity complexes because Crumbs3 assists in the recruitment of aPKC to the forming apical membrane and interference with their function can lead to the formation of a no-lumen or multiple-lumen phenotype at the two-cell stage.

INTRODUCTION

During kidney development, cells of the metanephric mesenchyme undergo massive morphological changes to form the renal vesicle, an epithelial structure surrounding a central lumen (Saxen, 1987). This process is termed mesenchymal-to-epithelial transformation and is tightly controlled at the transcriptional level (Boutet *et al.*, 2006; Thiery and Sleeman, 2006). The induction of the epithelial lumina is felt to depend on the induction of several polarity genes (Ikenouchi *et al.*, 2003; Martinez-Estrada *et al.*, 2006; Whiteman *et al.*, 2008), but exactly how the products of these polarity genes lead to initial lumen formation is still unclear. Several tissue culture models have been used to identify mechanisms underlying lumen formation (O'Brien *et al.*, 2002). Among these, cyst-formation and tube-formation assays allow the study of epithelial lumen formation de novo. It is generally believed that lumen formation is related to the formation and localized positioning of apical membrane, although additional mechanisms like apoptosis have been demonstrated to play a role in several contexts (Lubarsky and Krasnow, 2003). In Madin-Darby canine kidney (MDCK) cells, it has been shown that single epithelial cells (ECs) embedded in extracellular matrix (ECM) express apical proteins on their plasma membrane. These are thought to be endocytosed during the subsequent cell divisions, to form vesicular apical compartments (VACs) and to be exocytosed at the position of the forming lumen (Martin-Belmonte and Mostov, 2008). In this model, lumen formation has been shown to be completed at the four-cell stage. Others have reported lumen formation already in two- to three-cell aggregates, although underlying mechanisms remain elusive (Ferrari *et al.*, 2008; Jaffe *et al.*, 2008).

To successfully generate an apical lumen, ECs must acquire apicobasal polarity (Martin-Belmonte and Mostov, 2008). During the initiation of polarization, it is generally believed that phosphorylation-dependent mutual exclusion of apical and basolateral proteins leads to the separation of distinct apical and basolateral domains (Shin *et al.*, 2006). At the boundary between both domains mammalian ECs form a tight junction (TJ), serving not only as a tight intercellular seal, but also as a reinforcement of membrane polarity (Shin *et al.*, 2006). Apicobasal polarity is regulated by three evolutionarily conserved protein complexes, namely the apical Crumbs and Par complexes and the basolateral Scribble complex. In fact, in cyst-formation assays, interference with the proper regulation of polarity proteins leads to the generation of either multiple lumina or no lumen at all, as demonstrated for Crumbs3 (Crb3; Straight *et al.*, 2004; Shin *et al.*, 2005; Martin-Belmonte *et al.*, 2007; Torkko *et al.*, 2008; Schluter and Margolis, 2009). Crumbs (Crb) proteins have been demonstrated to be important determinants of apical membrane identity (Wodarz *et al.*, 1995; Lemmers *et al.*, 2004a; Fogg *et al.*, 2005; Omori and Malicki, 2006; Fan *et al.*, 2007). Thus it is tempting to speculate that polarity proteins are the master regulators for the formation of a lumen with a central role for Crb in the definition of the first apical membrane and subsequent lumen.

Although the knowledge of proteins involved in apicobasal polarity and lumen formation is growing, the mecha-

This article was published online ahead of print in *MBC in Press* (http://www.molbiolcell.org/cgi/doi/10.1091/mbc.E09–02–0137) on September 23, 2009.

Address correspondence to: Ben Margolis (bmargoli@umich.edu).

Abbreviations used: EC, epithelial cell; ECM, extracellular matrix; TJ, tight junction; VAC, vacuolar apical compartment.

nisms underlying the initial formation of a solitary lumen are not yet well characterized. Here we report that a single MDCK cell forms a cyst with a Crb3a-positive lumen during the first cell division. We demonstrate that the initial apical membrane gets established during and after cytokinesis through delivery of a Crb3-positive membrane from apical recycling endosomes that are trafficked along the mitotic spindle apparatus. The definition of the apical membrane eventually gives rise to the first lumen, because Crb3 knockdown reduces the size of the formed lumina or abolishes lumen formation altogether. Finally, Crb3 assists in the recruitment of Par–aPKC complex proteins to the forming apical membrane, where they serve to reinforce apical identity.

MATERIALS AND METHODS

Antibodies and Chemicals

Rabbit polyclonal Crb3a, rabbit polyclonal PATJ, and rabbit polyclonal PALS1 have been previously described (Roh *et al.*, 2002; Makarova *et al.*, 2003). Rabbit polyclonal canine Prominin-1 antibody was raised against the peptide CKLAKYYRRMDSEDVYD (100% identical to human), coupled to KLH. Rabbits were immunized at Proteintech Group (Chicago, IL). Mouse monoclonal GP135 antibody was a gift from George Ojakian (State University of New York). Mouse monoclonal α-tubulin, mouse monoclonal polyglutamylated-tubulin, mouse anti-Flag M2, mouse monoclonal γ-tubulin antibodies, nocodazole, and cytochalasin B were purchased from Sigma (St. Louis, MO). Mouse monoclonal pan-Rab11 was purchased from BD Biosciences (San Jose, CA). Rat polyclonal E-cadherin, mouse monoclonal ZO-1, and Alexa Fluor–conjugated secondary antibodies, DAPI, and phalloidin-rhodamine were purchased from Invitrogen (Carlsbad, CA). Atypical protein kinase Cζ (aPKCζ) myristoylated pseudosubstrate was purchased from Calbiochem (San Diego, CA).

Constructs and Cell Lines

GFP-Crb3a constructs. The Crb3a cDNA was described previously (Makarova *et al.*, 2003). Green fluorescent protein (GFP) was cloned into human Crb3a extracellular domain according to standard procedures. Briefly, an ectopic EcoRV site was inserted into Crb3 via site-directed mutagenesis (primer sequence: GCACTGTTTTGCCTTCATCCACCAGCTCCAGCTCC**GATATC**AACCTGCGTCCAGAAGCCATCACTGCTATCATCG), GFP was amplified via PCR and ligated in-frame into the EcoRV site in Crb3a. The whole construct was subcloned via PCR into the BamHI and ClaI sites of pRevTRE vector (Clontech, Mountain View, CA). Crb3a ΔERLI was cloned through PCR from pRevTRE GFP-Crb3a and cloned BamHI/ClaI into pRevTRE.

mCherry-E-cadherin construct. mCherry was PCR-amplified from pmCherry-N1 (Clontech; primer forward: TTTTGAATTCCTCGAGGGCGGCATGGTGAGCAAGGGCGAGGAGG, primer reverse: TTTTAAATTTCTACTTGTACAGCTCGTCCATGC) and digested with ApoI. pQCXIP (Clontech) was digested with EcoRI and ligated with the PCR product. E-cadherin was PCR-amplified (primer forward: TTTTGCGGCCGCCCACCATGGGCCCTTGGAGCCGCAGC, primer reverse: TTTTCTCGAGGCCTCCGTCGTCCTCGCCGCCTCCGTACATGTC), digested NotI/XhoI, and ligated into the NotI/XhoI-digested modified pQCXIP.

Crb3 knockdown cell lines have been previously described (Whiteman *et al.*, 2008). The second Crb3 target sequence used for Supplemental Figure S7 is GCCATCACTGCTATCATTG. Briefly, hairpin constructs against canine Crb3 mRNA were cloned into the pSiren-RetroQ (Clontech) vector system and transduced into MDCK cell lines. The cells were selected with 5 μg/ml puromycin for 2 wk. Knockdowns were confirmed by immunofluorescence and Western blotting.

PCR of Rab11a was done from a complete H.s. Rab11a EST (Invitrogen Clone ID: 5792753). H.s. Flag-Rab11a was cloned using the following PCR primers: Forward primer: TTAATT GGATCC CCACC ATG GAT TAC AAG GAC GAC GAT GAC AAG GGA GGC GGC ACC CGC GAC GAC GAG T; Reverse primer: TTTT GAATTC TTA GAT GTT CTG ACA GCA CTG CAC CTT TG. Primers were engineered to insert a BamHI restriction site followed by a Flag-epitope sequence at the 5′ end and an EcoRI restriction site at the 3′ end via PCR. H.s. Flag-Rab11a was cut with the appropriate restriction enzymes and ligated into pQCXIN (Clontech) for stable transduction into GFP-Crb3a Clone 7 cells and selected using 200 μg/ml Hygromycin (Invitrogen) and 600 μg/ml G418 (Invitrogen). Flag-Rab11a S25N (dominant negative) and Flag-Rab11a Q70L (constitutively active) mutants were made via site-directed mutagenesis using Pfu Turbo (Stratagene, La Jolla, CA). The following primer sequences were used for mutagenesis: S25N, forward: CCTTATTGGAGATTCTGGTGTTGGAAAGAATAATCTCCTGTCTCGATTTACTCGAAATGAG; and reverse: CTCATTTCGAGTAAATCGAGACAGGAGATTATTCTTTCCAACACCAGAATCTCCAATAAGG; Q70L, forward: GCACAGATATGGGACACAGCAGGGCTAGAGCGATATCGAGCTATAACATCAGCATATTATCG; and reverse: CGATAATATGCTGATGTTATAGCTCGATATCGCTCTAGCCCTGCTGTGTCCCATATCTGTGC. All sequences were verified at the University of Michigan Automated Sequencing Core.

Tissue Culture and Cyst Formation Assay

MDCKII cells were cultivated in DMEM (Invitrogen) supplemented with 10% FBS, 100 U/l penicillin, and 100 U/l streptomycin (Invitrogen). For Geltrex cyst assays, 80–90% confluent cells were detached with enzyme-free PBS-based cell dissociation buffer (Invitrogen) for 30 min, resuspended in DMEM with 2% Geltrex (Invitrogen), and seeded on a 100% Geltrex base in eight-well chamber coverslips (Labtek, Thermo Fisher Scientific, Rochester, NY) using 250 μl of 2×10^4 cells/ml for each well. Cells were fixed with 4% paraformaldehyde after periods of 12 h to 6 d. Tissue culture medium was replaced every 3 d.

Immunofluorescent staining of cysts in Geltrex was carried out in chamber coverslips. After fixation, samples were permeabilized with 0.1–0.5% SDS in PBS or 0.1% Triton X-100 in PBS. Samples were blocked in PBS plus 2% goat serum (PBSG). Primary antibody staining was performed in PBSG for 36 h. After four 30-min washes in PBSG, secondary antibody with DAPI and/or phalloidin-rhodamine in PBSG was added overnight. After four 30-min washes in PBSG, cells were analyzed by confocal laser microscopy (FV500, Olympus, Center Valley, PA). Three-dimensional reconstruction was performed with Volocity software (Perkin Elmer-Cetus, Waltham, MA). Live-cell imaging was performed on a Deltavision RT microscope (Olympus) and reconstructed with Imaris software (Bitplane Scientific Solutions, Saint Paul, MN). Cyst-assays in collagen were performed as previously described (Shin *et al.*, 2005).

For immunofluorescent staining of cells grown in monolayers, cells were grown on six-well Transwell filters (pore size 0.4 μm, Corning Costar, Lowell, MA). The filters were cut out, fixed in 4% paraformaldehyde for 1 h, permeabilized in 0.1–1% SDS or 0.1% Triton X-100, blocked for 1 h in PBSG, and stained with primary antibody overnight. After three 10-min washes on the shaker, cells were probed with secondary antibody plus DAPI for 2 h. Filters were transferred onto glass slides, and after addition of Prolong Gold antifade reagent (Invitrogen) covered under glass coverslips, and analyzed by epifluorescence (Eclipse TE2000-U, Nikon Instruments, Melville, NY) or confocal (FV500; Olympus) microscopy.

Western Blotting

Western blots were performed according to standard procedures. Briefly, one 10-cm dish of cells was lysed in 500 μl RIPA buffer (20 mM Tris, 150 mM sodium chloride, 5 mM EDTA, 10 mM sodium phosphate, 10% [vol/vol] glycerol, 1% [vol/vol] NP40, 1% [m/v] sodium deoxycholate, and 0.1% [m/v] SDS). Protein lysate, 50 μg, was separated on a 10% SDS-PAGE gel. Western blot transfers were performed according to standard procedures. The membranes were blocked with 5% BSA in TBS at 4°C overnight, probed with primary antibody for 1 h, washed three times for 10 min with TBS + 0.05% Tween (TBST), reprobed for 1 h with horseradish peroxidase–conjugated secondary antibody (GE Healthcare, Piscataway, NJ) in 5% dry milk in TBST, and washed again three times in TBST. Chemiluminescent exposure was performed with ECL or ECL Pico (Thermo Fisher Scientific, Rockford, IL).

RESULTS

Crumb3 exists in two splice isoforms: Crb3a and Crb3b. The carboxy-terminus of Crb3a ends in the sequence ERLI and this sequence binds to Pals1 as well as Par6 and is an evolutionarily conserved determinant of apical identity (Wodarz *et al.*, 1995; Makarova *et al.*, 2003; Lemmers *et al.*, 2004a; Omori and Malicki, 2006). The carboxy-terminus of Crb3b ends in the sequence CLPI, and this isoform binds to importins but its role in epithelial cells is not as well understood as Crb3a (Fan *et al.*, 2007). Knockdown of Crb3, in MDCK cells leads to a "no lumen" phenotype when the cells are grown in three-dimensional culture (Torkko *et al.*, 2008).

To further investigate the role of Crb3a during MDCK cyst formation, we cloned GFP-Crb3a into a Tet-inducible plasmid where we could control expression, because overexpression of Crb3a can disrupt apicobasal polarity (Figure 1A; Roh *et al.*, 2003). Using this plasmid in the absence of Tet induction, the basal expression level of the vector was sufficient to drive GFP-Crb3a expression at low levels. We obtained MDCKII clones with varying expression levels of GFP-Crb3a (Figure 1B).

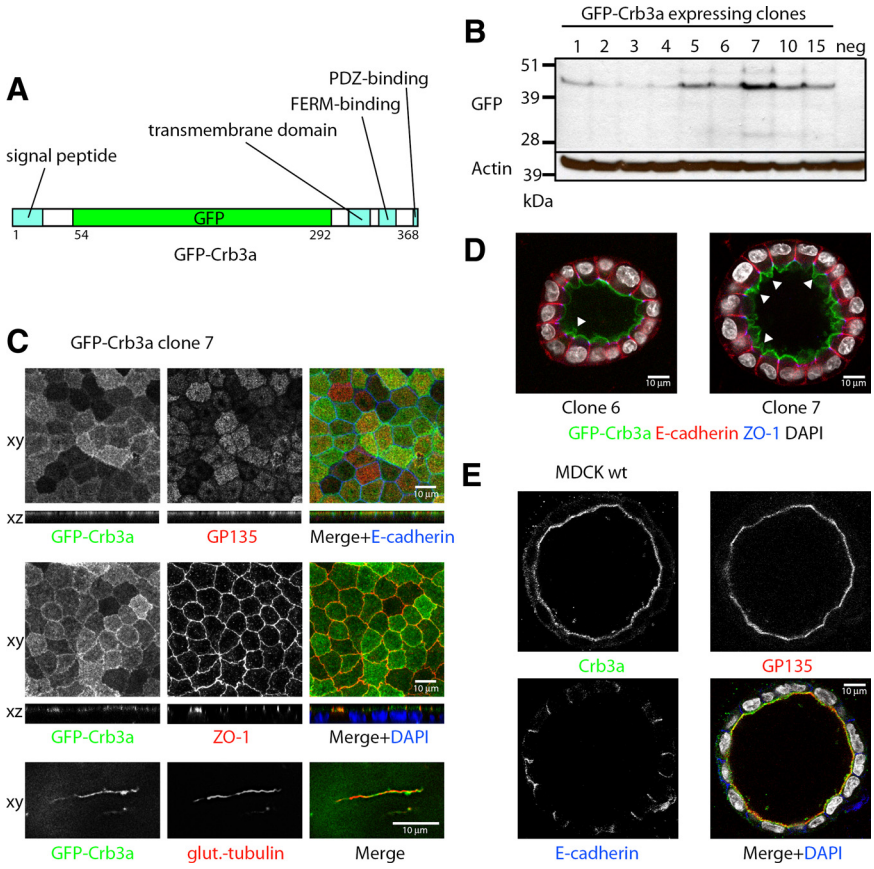

Figure 1. GFP-Crb3a expression in MDCKII cysts. (A) GFP-Crb3 construct. GFP-Crb3a was cloned into the tetracycline-inducible pRevTRE and virally transduced into wild-type MDCKII cells. (B) Western blot of GFP-Crb3a–expressing clones. MDCKII cells were infected with pRevTRE GFP-Crb3 and selected for 2 wk to generate a stable cell line. Clones were isolated, grown for 3 d, lysed in RIPA buffer, and analyzed by Western blot. The basal GFP-Crb3a expression in the absence of induction was sufficient to yield acceptable protein levels. (C) GFP-Crb3a localizes to the apical membrane, TJs, and cilia. MDCKII cells were grown on transwell filters for 4 or 7 d to obtain cilia, fixed, and costained with GP135, ZO-1, E-cadherin, or polyglutamylated tubulin. (D) Overexpression of GFP-Crb3a increases the size of the apical membrane domain. GFP-Crb3a–expressing MDCKII clones were embedded in collagen as previously described (Straight *et al.*, 2004), grown for 7 d, fixed, and stained for the indicated markers. Clone 6 is a low-level expresser and only shows a moderate expansion of the apical membrane (arrowhead), whereas clone 7 expresses GFP-Crb3a at a higher level and displays folds of surplus apical membrane on the luminal side (arrowheads). (E) MDCKII wild-type cells grown in collagen for 7 d possess a flat apical membrane positive for endogenous Crb3 and GP135.

GFP-Crb3a Localizes to the TJ and Apical Domain as well as Cilia and Promotes the Expansion of the Apical Domain

When grown on Transwell filters, MDCK cells form monolayers. As already reported GFP-Crb3a localizes to the apical membrane domain (Roh *et al.*, 2003), indicated by colocalization with the apical marker GP135, to the TJ, shown by colocalization with zonula occludens protein 1 (ZO-1), and to cilia, colocalizing with the cilia marker polyglutamylated tubulin (Figure 1C). This localization pattern was independent of the GFP-Crb3a expression level (data not shown).

When grown in collagen for 8 d, the cells form cysts with a single lumen (Figure 1D). Interestingly and in accordance with previous reports (Wodarz *et al.*, 1995; Lemmers *et al.*, 2004b; Omori and Malicki, 2006), increasing amounts of exogenous Crb3a induces apical membrane expansion, leading to apical membrane folding. (Figure 1D, arrowheads). In comparison, MDCK wild-type cells present a flat apical membrane when stained for endogenous Crb3a (Figure 1E).

The First MDCK Cell Division Creates a Cyst with a Crb3a-positive Apical Membrane

Because low-level expression of GFP-Crb3a allows cyst formation with solitary lumina, we set out to use this system for examining early stages of cyst formation. It was previously reported that the presence of laminin in the extracellular matrix had an influence on the speed of polarization and thus on the mechanism of lumen formation (Martin-Belmonte *et al.*, 2008). Thus we used a Geltrex (Invitrogen)-based cyst-formation assay, which has the advantage of growth-factor reduction, increasing the reproducibility of the experimental results. We embedded the cells into the ECM and fixed and stained them after 12–24 h of incubation (Figure 2). Through nonenzymatic cell detachment before embedding, we protected the GFP tag, which was located in the extracellular region of Crb3a, but still obtained a predominant single cell suspension (Supplemental Figure S1, A and B). MDCK cells were not cell cycle synchronized, so that all stages of the cell cycle can be visualized at a single time point at 12 h, whereas at 24 h cells had formed predominantly two-cell aggregates. The total amount of observed structures at 24 h was only insignificantly reduced compared with directly after embedding, suggesting that the observed two-cell stages were derived from cell divisions and not migrational and adhesion events (Supplemental Figure S1, A and B). Cells were stained for α-tubulin to determine the mitotic stage and for E-cadherin to visualize cell adhesions (Figure 2, A–C, Supplemental Figure S1, C–E).

During early stages (prepro- to metaphase) of the first cell division, GFP-Crb3a localized primarily intracellularly to the area of the α-tubulin–positive spindles (Figure 2A, Supplemental Figure S1C). At later stages of the first cell division, GFP-Crb3a localized to both cell poles (Figure 2B, Supplemental Figure S1D). With further progression of the telophase stage (as visualized by the developing midzone microtubule bundle), increasing amounts were visible on the side of the newly developing nuclei facing the opposite daughter cell (Figure 2B, outlined arrows) and in some cases became apparent at the tip of the midzone microtubule bundle (Figure 2B, bold arrows, Supplemental Figure S1D). In late telophase and two-cell stages, GFP-Crb3a plasma membrane staining became visible at the membrane between the two daughter cells (Figure 2, B and C). Apparent intracellular Crb3a-positive structures disappeared with further develop-

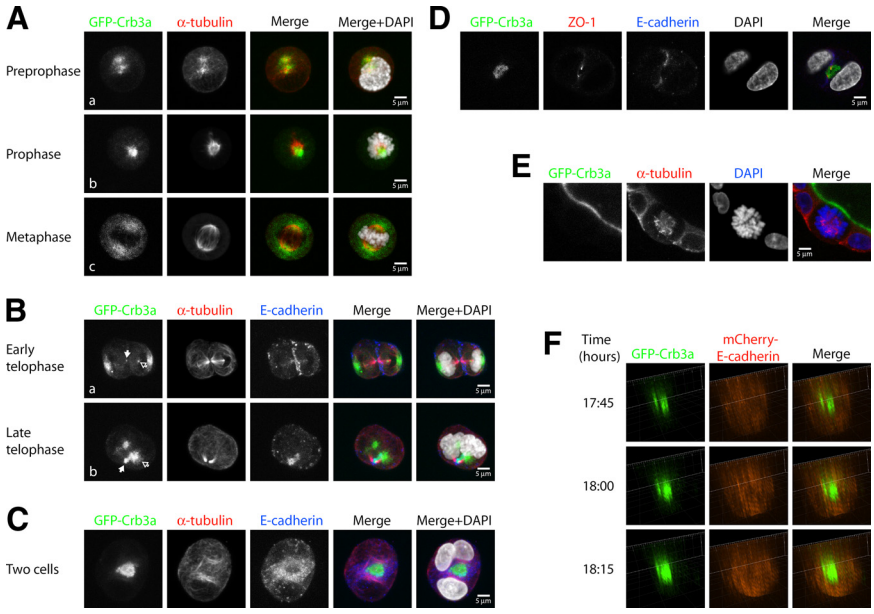

Figure 2. Lumen formation occurs during the first cell division of ECM-embedded MDCKII cells through positioning of apical membrane in the plane of division. (A–C) GFP-Crb3a–expressing (green) MDCKII cells were grown as single-cell suspensions in Geltrex-containing medium and were fixed at 12 h (for mitotic stages) or 24 h (for two-cell stages) after embedding. Cells were stained for E-cadherin (blue), α-tubulin (red), and DAPI (gray) and analyzed by confocal laser microscopy. (A, collapsed Z-stacks) During early stages of cell division GFP-Crb3a localizes to cytosolic compartments located around the mitotic spindle apparatus and partitions to both sides of the condensing nucleus during metaphase. (B, collapsed Z-stacks) At later mitotic stages, it relocates from a position at the lateral side of the nucleus (subpanel a) to the medial side of the two new daughter nuclei (outlined arrows) and finally forms a nascent lumen in the plane of the cell adhesion at the two-cell stage (C, collapsed Z-stacks). Note that GFP-Crb3a is evident at the tips of the midzone microtubule bundles (B, subpanels a and b, white arrows). (D) Single Z-section of a GFP-Crb3a–expressing two-cell stage, costained against ZO-1 (red) and DAPI (gray). (E, single Z-section) GFP-Crb3a only locates to spindle poles during early but not late cell divisions. GFP-Crb3a–expressing MDCKII cells in Geltrex-containing medium grown from single-cell suspensions were fixed after 8 d and stained for α-tubulin (red) and DAPI (blue). (F) Live-cell imaging of lumen formation during MDCKII cell division. MDCKII cells were sequentially virally transduced with GFP-Crb3a (in pRevTRE) and mCherry-E-cadherin (in pQCXIP). Images were three-dimensionally reconstructed at individual time points. The adhering membranes between two-daughter cells are displayed in side view, showing an emerging Crb3a-positive apical lumen.

ment of the apical membrane. This led us to speculate that Crb3a-positive vesicles traffic along microtubular routes to their subapical destination, where they arrive during telophase and are subsequently exocytosed to reinforce the initially aggregated apical membrane.

During the subsequent interphase, the developed two-cell structure possesses an emerging lumen with apical membrane identity, as shown by GFP-Crb3a localization (Figure 2C, Supplemental Figure S1E). This emerging lumen is surrounded by a ZO-1–positive TJ (Figure 2D). Both cells adhere through an E-cadherin–positive adherens junction surrounding the TJ (Figure 2, C and D, and Supplemental Movie 1). Staining performed with Crb3a-specific antibody confirmed these results (Supplemental Figure S2A). These data clearly demonstrate that dividing MDCK cells form a solitary lumen already at a two-cell stage. Interestingly, no more Crb3a trafficking to the spindle poles occurs at later cell divisions, promoting the idea that this trafficking mechanism is unique to the early cell divisions of MDCK cells (Figure 2E). Also, the functionality of this mechanism does not depend on the type of extracellular matrix, because MDCK cell divisions produce lumina as well, when grown in collagen type I (data not shown). This is in accordance with a previous report demonstrating lumina in MDCK two-cell aggregates when suspended in collagen, although cell divisions had not been observed in this context (Ferrari *et al.*, 2008).

To further delineate the sequence of events leading to early lumen formation, we sequentially coinfected the GFP-Crb3a MDCK cells with mCherry-tagged E-cadherin. In addition to the typical GFP-Crb3a staining, these cells display lateral mCherry-E-cadherin staining and maintain their ability to form hollow cysts (Supplemental Figure S, 3A and B). We embedded these double-fluorescent cell lines into ECM, performed live-cell imaging for 24 h, and reconstructed the dataset three-dimensionally (Figure 2F, Supplemental Figure S3C). The figures show the time after embedding into the ECM with live-cell imaging beginning 6 h after embedding. Single cells were chosen, as judged by size, GFP-Crb3a and mCherry- E-cadherin staining (Supplemental Figure S3C).

At early time points, accumulated GFP-Crb3a is seen in intracellular organelles. Images in Figure 2F focus on the plane between the two daughter cells initially formed by E-cadherin accumulation. At time 17:45 (h:min), regions were detectable where Crumbs3a was concentrated in patches that excluded E-cadherin. Subsequently, GFP-Crb3a intensity increased at the forming apical domain. Additionally, GFP-Crb3a–positive structures can be seen in proximity of the eventual lumen (Figure 2F). At time 19:00, a fully developed hollow GFP-Crb3a–positive emerging lumen is visible, excluding mCherry-E-cadherin, and indicating the completion of the first mitosis (Supplemental Figure S3C). In this system, however, recycling endosomes proved difficult to observe because of high cell motility at the one- to two-cell stage, causing structures to often leave the focal plane.

In mature cysts, Crb3a colocalizes with other apical proteins like GP135 (Figure 1E). To examine whether Crb3a colocalizes with GP135 in the previously characterized Crb3a-positive endogenous compartments, we performed costainings during the first MDCK cell division. Indeed, GFP-Crb3a as well as endogenous Crb3a and GP135 show a strong colocalization in these intracellular structures as well as at the emerging lumen (Figure 3A and Supplemental Figure S2A).

The process of Crb3a-positive membrane trafficking from the plasma membrane of single cells to internal compartments and back to the forming apical membrane is reminiscent of recycling endosomal trafficking, as published for Rab11-positive endosomes (Hobdy-Henderson *et al.*, 2003). Rab11-positive endosomes and Rab11 family–interacting proteins have been implicated in the biosynthetic trafficking

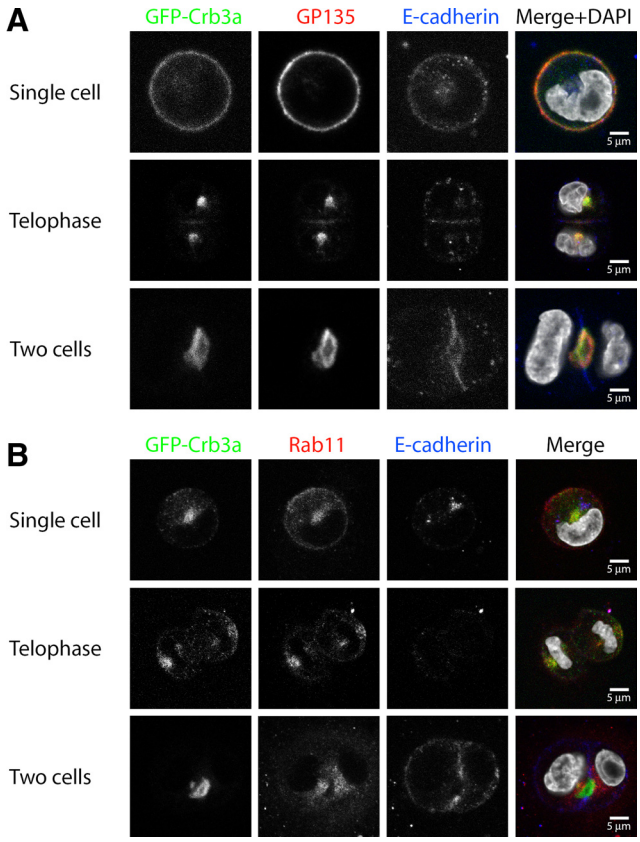

Figure 3. Costaining of GFP-Crb3a with GP135 and Rab11 (single Z-sections). GFP-Crb3a–expressing MDCKII cells were embedded in Geltrex as described, fixed at different times, and costained for GP135 (A) or Rab11 (B). (A) GP135 can colocalize with GFP-Crb3a–positive compartments during MDCK cell division. (B) GFP-Crb3a colocalizes with Rab11.

and recycling of apically targeted proteins (Wang *et al.*, 2000; Cresawn *et al.*, 2007). Indeed, GFP-Crb3a–positive intracellular compartments show a strong staining for Rab11 during this first cell division (Figure 3B and Supplemental Figure S2B). At the two-cell stage, when Crb3a becomes localized to the newly formed apical membrane, it loses colocalization with Rab11, which remains in a subapical area, indicating complete delivery of Crb3a to the newly formed apical surface.

Crb3a Trafficking Depends on the Microtubular Cytoskeleton during First Cell Division

Because Crb3a is a transmembrane protein and redistributes along the mitotic spindle during this first cell division (Figure 2, A–C), we hypothesized that the tubulin cytoskeleton directs Crb3a vesicles during initial partitioning and formation of apical membrane between the two daughter cells. Interestingly, and in contrast to a previous report (Ferrari *et al.*, 2008), GFP-Crb3a does not colocalize with actin during the initial cell division before the two-cell stage (Figure 4A).

Because nocodazole treatment prevents cell division altogether, it is impossible to test the microtubular role for Crb3a trafficking during cell division, as seen at 36 h after seeding (Figure 4B; phenotype occurred in all observed cells). Cells treated with nocodazole fail to divide, whereas many cysts in the DMSO-treated control have already reached the four-cell stage. Nevertheless, the nocodazole-treated cells often display vacuolar GFP-Crb3a–positive structures along the periphery, and these structures also possess the apical marker GP135, but not the basolateral protein E-cadherin, which often localizes in proximity to Crb3a-positive areas (Figure 4, B and C). Interestingly, most of the observed GFP-Crb3a–positive vesicles are negative for Rab11 (Figure 4C). We speculate that these vesicles might represent mature apical membrane, which have failed to be delivered to its proper destination.

To test the role of the actin cytoskeleton in Crb3a trafficking, we inhibited actin polymerization through cytochalasin B treatment. On cytochalasin B–mediated depolymerization of the actin cytoskeleton, cells are still able to produce mitotic spindles and undergo nuclear mitosis, but they lose the ability to undergo cytokinesis because of inhibition of contractile actin ring assembly (Figure 4D). Strikingly, GFP-Crb3a is still able to partition to the spindle poles under actin-depolymerizing conditions. Furthermore it retains its ability to traffic back to the medial side of the two daughter nuclei during anaphase. Because there is no efficient bundling of the midzone microtubules (Figure 4Dc, bold arrow) and no intercellular membrane where the endocytosed membrane could traffic to, GFP-Crb3a–positive vesicles accumulate in a broader area between the two daughter nuclei (Figure 4Dd). It is important to note that a majority of these vesicles do not colocalize with Rab11, but rather with GP135 (Supplemental Figure S4), pointing to a mature apical identity and underlining the notion that disruption of tubulin polymerization causes a defect of membrane-delivery, but not membrane maturation.

To further test the importance of Rab11-containing endosomes in cytokinetic membrane trafficking, we expressed wild-type, dominant active (Q70L), and dominant negative (S25N) Rab11a in GFP-Crb3a cells and then studied early apical membrane formation (Supplemental Figure S5). We found that dominant negative but not wild-type or dominant active Rab11a perturbed early apical membrane formation. At the two-cell stage, GFP-Crb3a could be seen localized to emerging lumens in the cells expressing control, wild-type, and dominant active Rab11a, whereas GFP-Crb3a was diffusely localized in the cells expressing dominant negative Rab11a. Taken together, our data suggest that during MDCK cell divisions, Crb3a gets internalized into Rab11-positive vesicles and is transported along microtubular routes to the newly forming apical membrane.

Members of the Crb3 Complex, But Not the Par3/Par6/aPKC Complex Colocalize with Recycling Endosomes during the First Cell Division

At the TJ, Crb3a forms an apical protein complex with PALS1 and PATJ (Wang and Margolis, 2007). The Par complex consists of Partitioning defective 3 (Par3), Par6, and aPKC, and both protein complexes are involved in the establishment and maintenance of apicobasal epithelial polarity (Wang and Margolis, 2007). Thus we were interested in investigating whether apical polarity proteins would traffic along the same route as Crb3a during the first MDCK cell division.

Indeed, PALS1 and PATJ colocalize with Crb3a in the cytoplasmic recycling endosomes, as seen for the GFP-tagged proteins and endogenous PALS1 (Figure 5, A and B, and Supplemental Figure S6). Interestingly, endogenous Par3 and aPKC cannot be found in these structures and only appear at the newly formed tight junction or lumen, respectively (Figure 5, C and D).

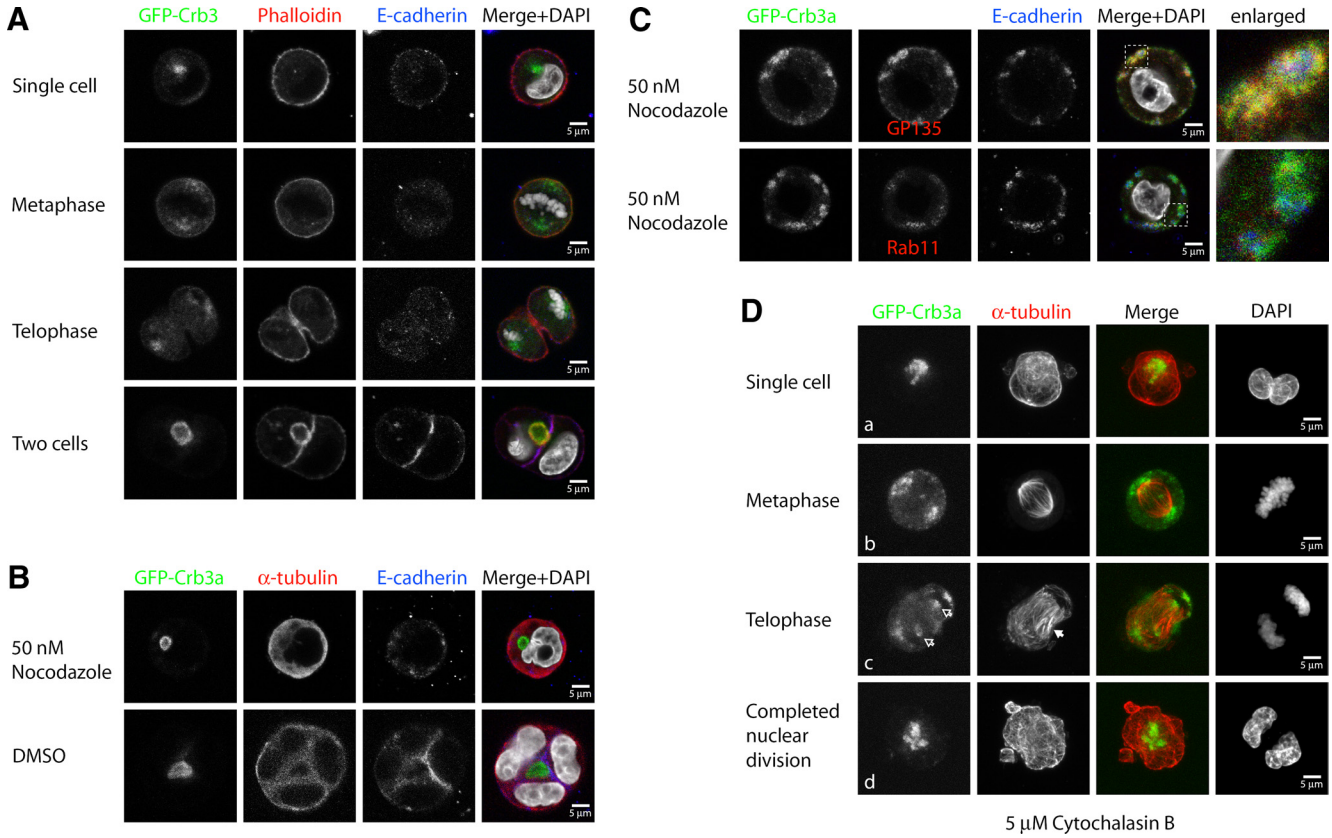

Figure 4. Internalization and trafficking of GFP-Crb3 is independent of actin polymerization. GFP-Crb3a–expressing MDCKII cells were embedded in Geltrex as described, fixed at different times, and stained with the indicated antibodies or phalloidin. For tubulin inhibition experiments (B and C, single Z-sections), the 2% Geltrex-containing medium was supplemented with 50 nM nocodazole or an equal volume of DMSO. Actin inhibition experiments (D) were performed in the presence of 5 μM cytochalasin B. (A) Control cells, single Z-sections. GFP-Crb3a does not colocalize with actin-positive structures until the nascent lumen is formed. (B) Inhibition of tubulin polymerization. At 36 h after embedding, uninhibited cells (DMSO) have mostly reached the four-cell stage, whereas nocodazole treatment inhibited cell division in all observed cells. (C) Nocodazole-treated cells did not form solitary lumina, but showed small diffusely distributed structures localizing adjacent to the plasma membrane. GFP-Crb3a–positive structures colocalize with GP135, but not E-cadherin or Rab11 (see enlarged parts of merged images). (D, collapsed Z-stacks) Cytochalasin-treated cells. Inhibition of actin polymerization with cytochalasin B does not impair internalization of GFP-Crb3a, its transport to the spindle poles and to the medial side of the two daughter nuclei (outlined arrows). The forming midzone microtubules (solid arrow) fail to get bundled as a result of the inhibited cytokinesis.

Knockdown of Crb3 Abolishes Lumen Formation at the Two-Cell Stage

Crumbs proteins have been implicated in the definition of apical membrane identity and in lumen formation (Wodarz *et al.*, 1995; Omori and Malicki, 2006; Torkko *et al.*, 2008). In mature MDCK cysts, Crb3a localizes to the apical membrane (Figures 1, D and E). Thus we were interested in examining whether and how Crb3a is involved in the initial lumen formation of dividing MDCK cells. To address this question, we established Crb3 short hairpin RNA (shRNA) knockdown MDCKII cell lines. After infection, we isolated clones, lysed them after 3 d, and analyzed protein expression by Western blotting (Supplemental Figure S7, A and B). Crb3a expression was significantly suppressed, whereas expression of PATJ, PALS1, aPKCζ, and the apical marker Prominin1 was unchanged. The expression of GP135 was reduced to some extent in some, but not of the cell clones compared with their controls (Supplemental Figure S7, A and B).

To assess the impact of Crb3 knockdown on the initial lumen formation, we embedded the cells into Geltrex as previously described and performed cyst-formation assays. Different stages of cell divisions were visualized by confocal laser microscopy (Figure 6A). At mature two-cell stages, we determined the average size of an early apical membrane or lumen—if present—at the attaching membranes between the two daughter cells in the control cell line. Lumen size could be judged by the size of GP135 enrichment with simultaneous E-cadherin exclusion. Early apical structures measured between 6 and 11 μm, as visualized by GP135 staining. Thus we grouped the acquired two-cell stage datasets into "no lumen," "small lumen" (≤5 μm) or "regular lumen" (>5 μm) phenotypes (quantification in Figure 6B and Supplemental Figure S7C). Although the control cells showed an average amount of 34% of regular-sized lumina and 13% of small lumina (Figure 6, Aa and B), Crb3a knockdown cell lines seemed to have lost their ability to form these early lumina almost completely. Clone 3 displayed a residual amount of 1.4% regular-sized lumina and 17.4% of small lumina (Figure 6, Ac and B). The residual two-cell stages had no GP135-positive membrane or lumen at all at the attaching membranes of the daughter cells, because E-cadherin staining was continuous (Figure 6Ab). Nevertheless, cytoplasmic submembranous GP135 accumulations were often present under the adhering membrane. Similar results were obtained for clone 7 and clone 22 (Figure 6B) and with a second hairpin (Supplemental Figure S7C). Al-

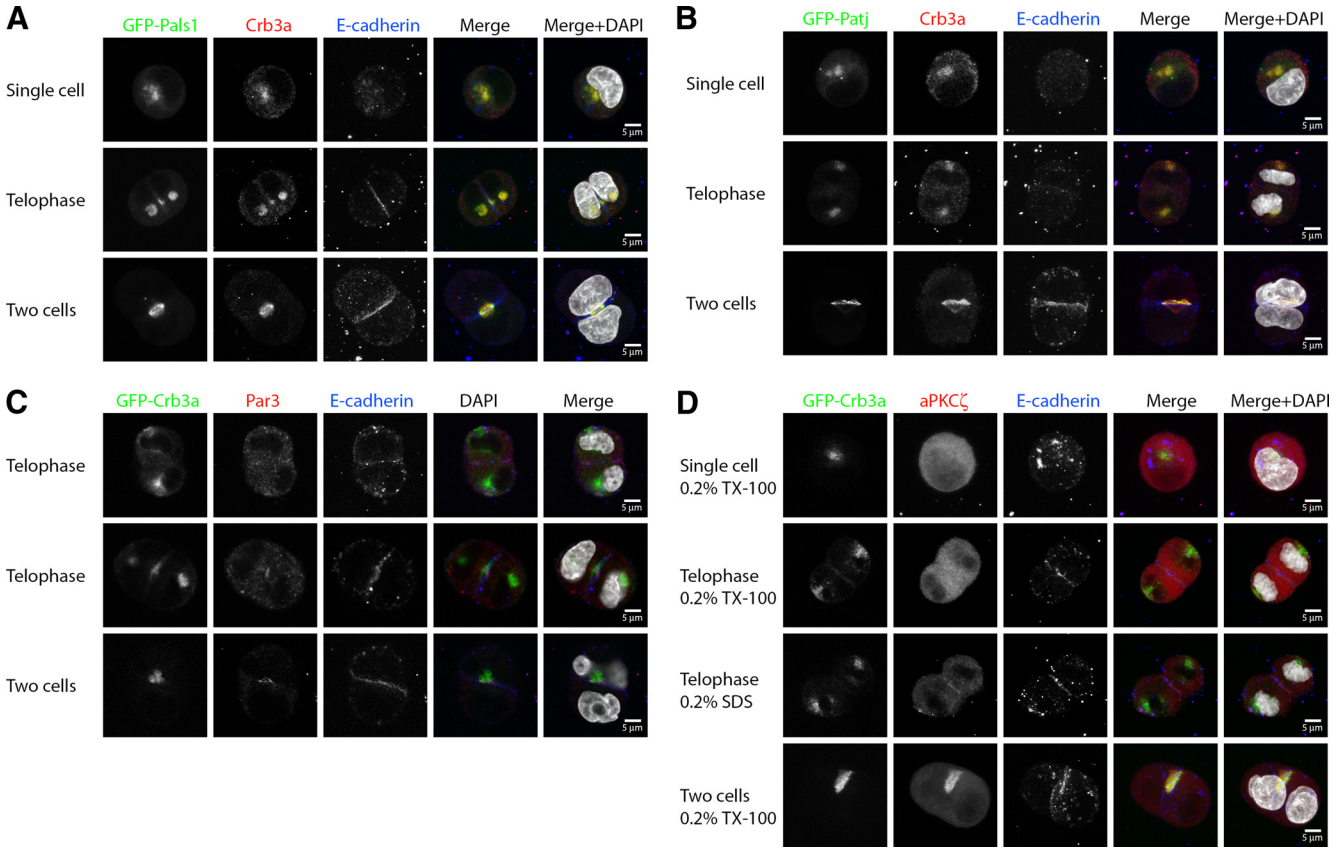

Figure 5. Members of the Crb3 complex, but not Par3–aPKC complex, are recruited to Crb3a-positive endosomes. MDCKII cells were embedded in Geltrex as previously described, fixed at different times, and stained with the indicated antibodies. Single Z-sections are displayed. (A and B) Exogenously expressed GFP-PALS1 and GFP-PATJ colocalized with Crb3a. (C and D) Par3 and aPKCζ do not initially colocalize with GFP-Crb3a, but get enriched at the newly forming TJ and/or apical membrane between the two daughter cells and at the emerging lumen.

though lumen formation was strongly impaired by Crb3 knockdown, the cellular uptake of GP135 and its partitioning to the spindle poles seems to be unaffected at early stages of cell divisions (Figure 6Ad), similar to wild-type MDCK cells (Figure 3A).

Members of the Crb3 complex have been shown to directly interact with members of the Par3/Par6/aPKC complex (Hurd *et al.*, 2003b; Lemmers *et al.*, 2004b). We previously reported that Crb3a was able to recruit Par6 to the membrane in unpolarized cells (Hurd *et al.*, 2003b). Thus we hypothesized that the delivery of Crb3a complex to the forming apical membrane might serve as an anchor recruiting Par3/Par6/aPKC to this location. Immunostaining of two-cell stages for aPKCζ in Crb3 knockdown cell lines reveal that little or no aPKCζ is present at the membrane between the two daughter cells, where lumen formation is absent (Figure 6Ab). At two-cell stages with residual lumen formation we found aPKCζ staining to be limited to the site of the small lumina, where it accumulated with high intensity (Figure 6Ac). Because apical membrane areas are strongly reduced in size and number, aPKCζ-positive areas are reduced to the same extent. This indicates that Crb3a-positive membranes might recruit aPKCζ, possibly through interaction with Par6, to the forming apical membrane.

GFP-Crb3a Rescue of Lumen Formation

The canine Crb3 short hairpin target sequences are directed against both canine Crb3a and -b isoforms. Because Crb3a shows the higher degree of conservation and has a well-established role in cell polarity, we generated GFP-Crb3a rescue cell lines of Crb3 shRNA interference (shRNAi) clone 3. After 2 wk of selection, the expression of the rescue constructs was determined by Western blotting (Figure 7A). Both full-length GFP-Crb3a (FL) and the truncated protein missing its PDZ-binding motif (ΔERLI) were expressed at similar levels. The knockdown of endogenous Crb3a was maintained in the empty vector control and in both rescue cell lines, compared with MDCK wild-type cells.

The generated cell lines were tested in the lumen-formation assay as described in *Materials and Methods,* fixed after 24 h, and stained for aPKCζ and E-cadherin. Two-cell stages were visualized through confocal microscopy, and lumen diameters were measured and statistically analyzed (Figure 7, B–D). Cell lines transduced with GFP-Crb3a FL showed a significant rescue with strong aPKCζ recruitment (Figure 7Bb), Par3 at tight junctions (Supplemental Figure S8), and lumen diameters predominantly >5 μm (Figure 7C), whereas control vector-transduced cells only showed a residual amount of lumen formation and aPKCζ staining similar to the results of the original knockdown clone (Figures 6, A and B, and 7, Ba and C). Interestingly, GFP-Crb3a ΔERLI-transduced cells showed a partial rescue of lumen formation, although the amount of lumina >5 μm was decreased (Figure 7, Bc and C). On average, full-length rescued cells possessed lumen diameters about 5.2 μm, whereas GFP-Crb3a ΔERLI presented lumen diameters averaging 3.2 μm

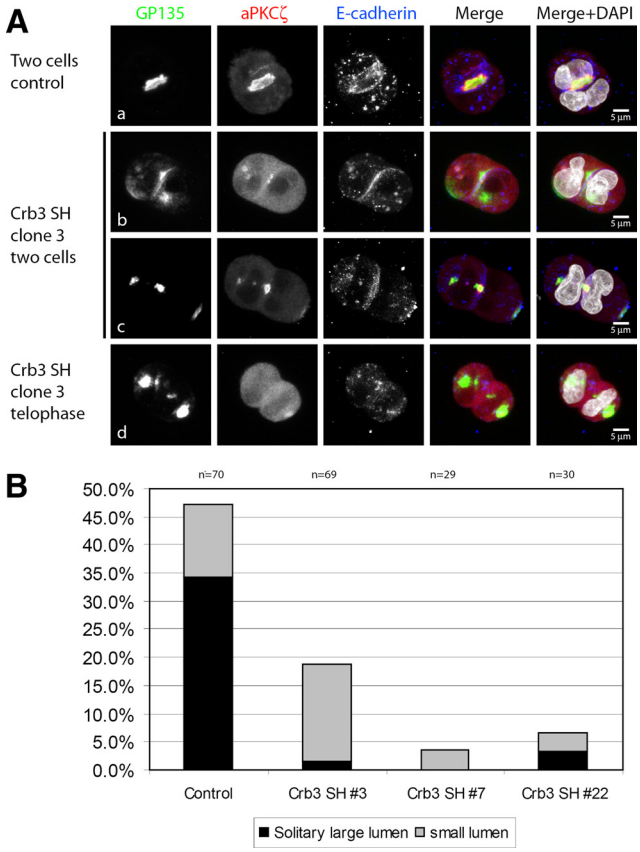

Figure 6. Crb3 is required for the formation of the first apical lumen and recruitment of aPKCζ. Crb3 shRNA knockdowns were prepared as previously described. Isolated cell clones were embedded in Geltrex, fixed after 24 h, and stained with the indicated antibodies. (A, collapsed Z-stacks) In contrast to Luciferase shRNA treated control cells (subpanel a) that formed regular solitary lumina (arrow) at the two-cell stage (lumen size >5 μm), Crb3-depleted cells formed two-cell stages with missing intercellular lumina, because E-cadherin staining is continuous (subpanel b) or strongly decreased lumen size (subpanel c). Knocked-down cells often formed intracytoplasmic accumulations of the apical marker GP135 (subpanel b), with a simultaneous accumulation of aPKCζ. Some cells with impaired lumen formation showed minimal accumulation of aPKCζ at attaching membranes between daughter cells (subpanel b). GP135 internalization was still functional in Crb3 knockdown cells (subpanel d). (B) Quantification of the phenotypes of three different clones. Lumina were quantified according to their size (lumina ≤5 μm were categorized as small). Results were acquired in three independent experiments.

(Figure 7D). Interestingly, the truncated construct failed to recruit aPKCζ efficiently in every observed case (Figure 7Bc). Taken together, our data suggest that the phenotype of the Crb3 knockdown is specifically caused by reduction of Crb3a, because GFP-Crb3a FL fully rescues the observed phenotype.

Inhibition of aPKCζ Impairs Apical Membrane Definition

We wanted to further test the role of aPKC in apical membrane determination. aPKC is a member of the Par polarity complex and is indispensable for the establishment of epithelial polarity in numerous systems (Shin *et al.*, 2006). aPKC has been shown to maintain epithelial polarity by phosphorylating and thus excluding basolateral proteins from the apical membrane domain, promoting apical identity (Plant *et al.*, 2003; Hurov *et al.*, 2004; Suzuki *et al.*, 2004). Inhibition of aPKCζ with myristoylated pseudosubstrate induces a multiple-lumen phenotype in mature MDCK cysts (Martin-Belmonte *et al.*, 2007). Thus we were interested if inhibition of aPKCζ would affect the formation of the nascent lumen already at the two-cell stage. Experiments were performed as described in *Materials and Methods.* aPKCζ pseudosubstrate was added to the Geltrex-containing liquid medium at the indicated concentration. First, we determined the maximal viable aPKCζ inhibitor concentration under the chosen experimental conditions. We found that a concentration of 100 μM is lethal for the majority of cells, whereas MDCK cells survive well at 50 μM, which we chose for the following experiments. At mature two-cell stages in untreated control cells, nascent GFP-Crb3a–positive lumina become evident surrounded by a single TJ, as seen for ZO-1 staining (Figure 8Aa). aPKCζ inhibition caused abnormal lumina as defined by formation of multiple lumina between the two daughter cells in some cases (Figure 8Ab, arrows, Supplemental Movie 2), but more frequently ectopic localization of GFP-Crb3a or ZO-1 in proximity to the emerging lumen (Figure 8Ac, arrowhead). Quantitative analysis of the phenotypes is provided in Figure 8B. We hypothesize that Crb3a recruits aPKCζ to the newly forming Crb3-positive apical membrane, where it serves to reinforce apical identity through the exclusion of basolateral proteins.

DISCUSSION

MDCK cyst formation has been used as a model for the study of epithelial cell polarity for several years but the underlying mechanisms regulating the emergence of the very first lumen remain unclear (O'Brien *et al.*, 2002). Lubarsky and Krasnow (2003) summarized data on lumen formation and concluded that lumen formation was related to the delivery of apical membrane. We demonstrate that MDCK cells can create apicobasal polarity and a primary lumen from a single symmetric cell division. A similar mechanism has been demonstrated before in zebrafish neurulation, where neuroepithelial cells divide during neural keel and rod formation, resulting in two separate cells with symmetric Par3 positioning surrounding a newly formed lumen (Tawk *et al.*, 2007). We propose that this might be a general mechanism represented in various types of epithelial cells.

Internalization, Partitioning, and Delivery of Crb3a-positive Membrane through Rab11-positive Endosomes Lead to Lumen Formation from MDCK Mitosis

During the first cell division, MDCK cells are able to internalize apical membrane components from their plasma membrane, partition them to the spindle poles of the newly forming nuclei, and finally deliver them to a membrane area between the two daughter cells, thus constituting a first lumen (Figures 2 and 3). We have found that the internalized fraction of Crb3a colocalizes with Rab11-positive endosomes during cell division (Figure 3B, Supplemental Figure S2B).

Rab GTPase family–positive recycling endosomes have been identified as important players of apical trafficking (van Ijzendoorn, 2006; Sato *et al.*, 2007; Nokes *et al.*, 2008). Especially the Rab11-family seems to play a central role in apical trafficking and consists of Rab11a, -11b, and -25 (Bhartur *et al.*, 2000). Rab11-positive recycling endosomes together with Rab11-FIP3 (Rab11 family–interacting protein 3) have also been implicated in membrane delivery that is required during cytokinesis and abscission. In interphase, proteins of the apical recycling endosomes localize to areas around centrosomes (Horgan *et al.*, 2004). During mitosis, Rab11a

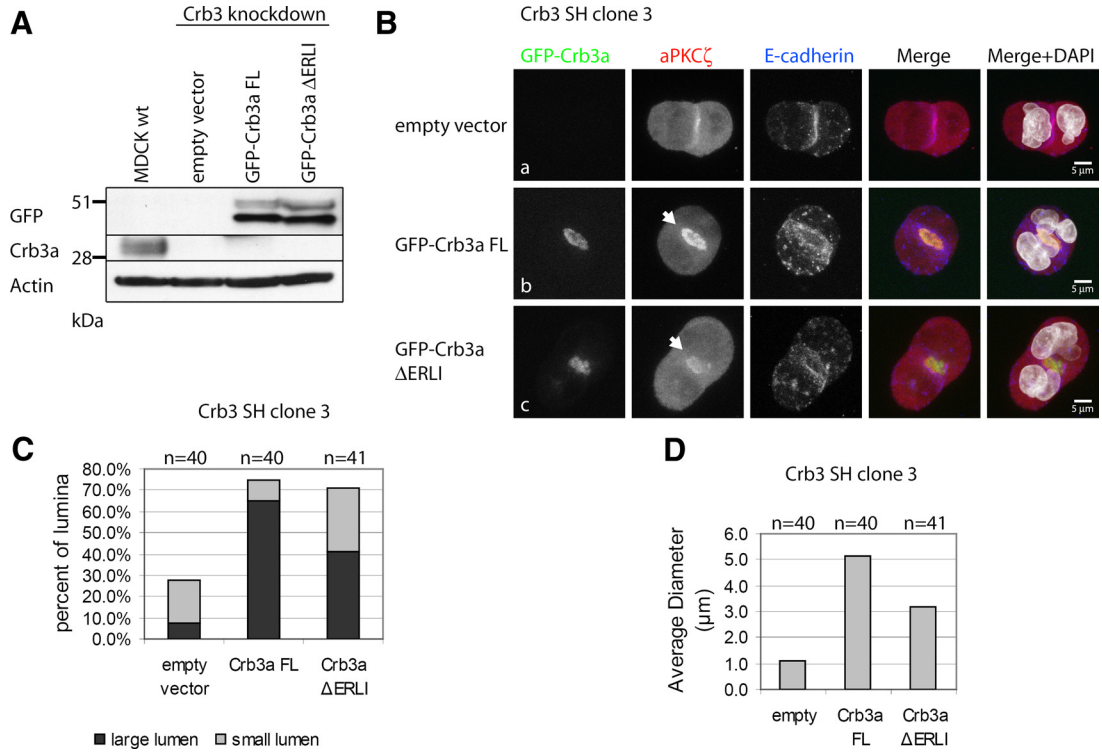

Figure 7. Expression of GFP-Crb3a rescues the knockdown of Crb3. Crb3 shRNA clone 3 was transduced with empty pRevTRE vector, pRevTRE GFP-Crb3a full-length (FL), or missing its PDZ-binding motif (ΔERLI). (A) Western blot of MDCK wild-type cells versus empty vector–infected cells shows a persisting knockdown of Crb3a. Probing with anti-GFP antibody reveals similar expression levels for FL and ΔERLI constructs. (B, collapsed Z-stacks) Empty vector–transduced cells presented primarily a no-lumen phenotype with minimal recruitment of aPKCζ to the site of cell adhesion similar to the original knockdown (subpanel a). Expression of GFP-Crb3a FL rescues lumen formation and aPKCζ recruitment (subpanel b). GFP-Crb3a ΔERLI expression partially rescues MDCK lumen formation with a smaller average lumen diameter, but not aPKCζ recruitment, which was minimal in all observed two-cell stages (subpanel c). (C) Quantification of phenotypes. Cells with a lumen size >5 μm were categorized as large lumen, and smaller sizes were counted as small lumen. GFP-Crb3a FL expression rescues lumen formation with predominantly large lumina. GFP-Crb3a ΔERLI-expression Crb3a shRNAi cells display a partial rescue with a greater number of small lumina. (D) The average lumen diameter is significantly smaller in ΔERLI-rescued cells (3.2 μm) compared with FL-rescued cells (5.2 μm).

aggregates near the spindle poles, and these aggregates are symmetrically inherited by both daughter cells (Hobdy-Henderson *et al.*, 2003). Thus it seems likely that the targeting of apical proteins such as Crb3a into Rab11-positive vesicles plays a role in the initial formation of the apical membrane and ongoing apical membrane trafficking. Indeed we were able to demonstrate that dominant negative Rab11a blocked GFP-Crb3a trafficking and formation of early apical membrane (Supplemental Figure S5).

In addition to colocalizing with Rab11, Crb3a accumulates at the end of the midzone microtubule bundle and colocalizes with it during telophase of the first MDCK cell division (Figure 2B). Live-cell imaging shows a strong increase in the initial GFP-Crb3a signal at the membrane between the two daughter cells at the end of cell division (Figure 2F, Supplemental Figure S3C). Together, these data lead us to speculate that Rab11-positive endosomes deliver apical membrane to the site of abscission, leading to the formation of the first lumen. Because the exact partitioning mechanism for apical recycling endosomes is still elusive, we performed costainings between GFP-Crb3a–positive aggregates and cytoskeletal proteins tubulin or actin, respectively. We found that at all stages of mitosis, GFP-Crb3a–positive compartments localize along or in proximity of the tubulin cytoskeleton (Figure 2, A–C). Conversely, we found that colocalization with actin only occurred at very early or late stages of mitosis (Figure 4A). Nocodazole-dependent inhibition of tubulin polymerization led to an impairment of nuclear division with vesicles of apical identity localized to random submembranous spots (Figures 4, B and C). In contrast inhibition of actin polymerization with cytochalasin B impaired cytokinesis but not nuclear division (Figure 4D). Crb3a partitioning to the opposite spindle poles was still intact despite actin inhibition, leading to the notion that the actin cytoskeleton is expendable for this process. This indicates that trafficking of Crb3a in early cell division is predominantly microtubule based.

Crb3 and Apical Membrane Identity

Although trafficking along distinct routes, both members of the Crb3– and Par–aPKC-complexes become enriched at the attaching membranes of the two daughter cells, in proximity of the midzone microtubules. All Crb3-complex members traffic in Rab11-positive endosomes along microtubular routes, whereas Par–aPKC complex members that distribute evenly throughout the cytoplasm in single MDCK cells get concentrated at the forming apical membrane without association with Rab11-positive compartments.

Crb3a has been shown to recruit Par6 to the membrane of unpolarized cells through a direct interaction; furthermore; a direct interaction between Pals1 and Par6 has been demonstrated (Hurd *et al.*, 2003b; Lemmers *et al.*, 2004b). At the

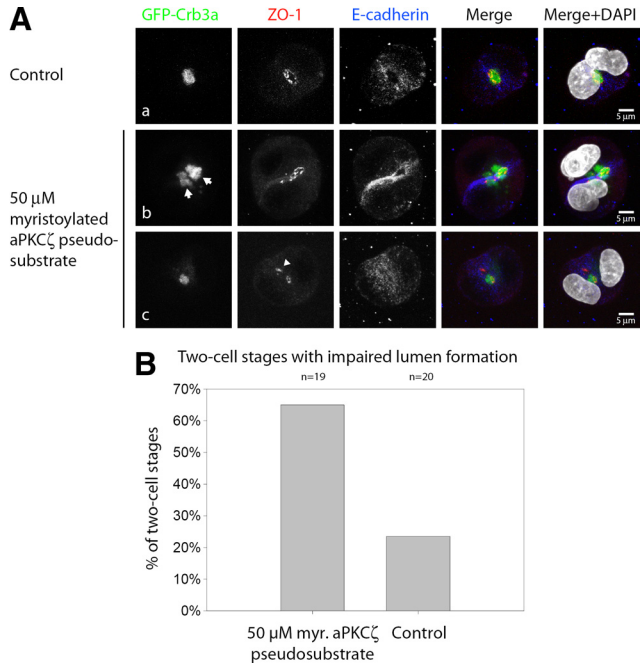

Figure 8. Inhibition of aPKCζ impairs the regulated formation of a solitary lumen at the two-cell stage. GFP-Crb3a–expressing MDCKII cells were embedded in Geltrex as described. In some specimens, myristoylated aPKCζ pseudosubstrate (Calbiochem) was added to the liquid medium as indicated. Cells were fixed 24 h after embedding and stained with the indicated antibodies. (A, collapsed Z-stacks) In untreated cells, the majority of two-cell stages showed regular lumen formation, (subpanel a), whereas inhibitor-treated cells either showed ectopic localization of apical or tight junction components (subpanel c arrowhead) or occasionally had more than one lumen (subpanel b, arrows). (B) Quantification of two-cell stages with impaired lumen formation (ectopic localization of apical or tight junction components or multiple lumina) in aPKCζ pseudosubstrate–treated cells versus untreated cells.

end of MDCK division in our experimental setup, Crb3a assists in recruiting aPKCζ to the site of the nascent apical lumen, because aPKCζ is limited to residual areas of lumen formation in Crb3 knockdown conditions (Figure 7). Furthermore, although both constructs could rescue lumen formation partially, GFP-Crb3a FL more efficiently recruited aPKCζ than GFP-Crb3a ΔERLI, and lumens were smaller in the GFP-Crb3a ΔERLI cells. GFP-Crb3a ΔERLI was able to partially rescue lumen formation despite its impaired ability to recruit aPKCζ (Figure 7). The partial rescue might be due to overexpression of GFP-Crb3a ΔERLI at levels above the endogenous Crb3a level. Residual endogenous Crb3a might also be responsible for small amounts of aPKCζ being recruited to the emerging lumen in these cells (Figure 7Bc). Another possible explanation would be that Crb3a may be able to exert its ability to expand the apical membrane even without its PDZ-binding motif. If this was true, a residual amount of endogenous Crb3a being able to interact with Pals1 and aPKC might be sufficient to generate a functional tight junction and recruit small amounts of aPKC. The fact that the average lumen diameter in GFP-Crb3a ΔERLI rescued cells is reduced may reflect the impaired ability of GFP-Crb3a ΔERLI to contribute to TJ formation, limiting the size of the apical domain (Figure 7D). Finally, we cannot exclude the possibility of overlapping mechanisms of aPKC recruitment and TJ formation, which might result in a partial rescue even when overexpressing C-terminally truncated GFP-Crb3a.

Interestingly, we find Par3 staining restricted to the emerging TJ, but not at the forming luminal membrane, indicating that Par3 is expendable for apical aPKCζ recruitment. In contrast to this, Horikoshi *et al.* (2009) find that the interaction between Par3 and aPKC is required for the delivery of apical membrane in calcium-switch assays. The authors also demonstrate that Par3 is not always associated with Par6-aPKC. Under low calcium conditions Par6 and aPKCλ, in contrast to Par3, accumulate in cytoplasmically located vacuolar apical compartments (VACs). VACs were described more that 20 years ago as a compartment displaying apical features such as microvilli and apical proteins, appearing in epithelial cells under low-calcium or low-confluency conditions or when cells are embedded into ECM, such as collagen or agarose (Vega-Salas *et al.*, 1987). In our lumen-formation assay, where cells get embedded into Geltrex containing laminin, we find only accumulation of Crumbs complex proteins, but not Par3 or aPKCζ in cyto-

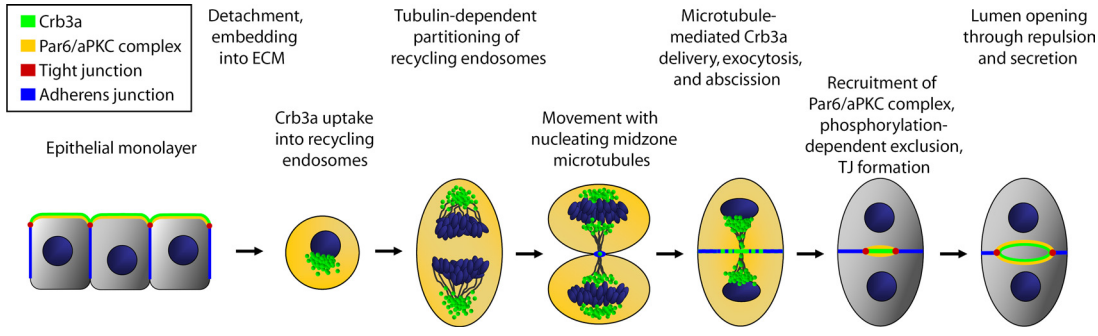

Figure 9. Model of MDCK lumen formation during cell division. Single cells embedded in extracellular matrix internalize Crb3-complex proteins into apical endosomal compartments. On formation of the spindle apparatus, the Crb3-complex members get transported to the spindle poles, whereas members of the Par–aPKC complex show a diffuse cytoplasmic localization. Crb3-complex proteins become apparent near newly nucleating microtubules that eventually form the midzone microtubules. The apical endosomes appear to get transported along the midzone bundle to the site of cytokinesis, where they are exocytosed. This lays the foundation for the formation of an apical membrane. Crb3a recruits aPKCζ through its PDZ-binding motif, most likely through interaction with Par6, to the forming apical membrane, where aPKCζ contributes to apical membrane identity through phosphorylation-dependent exclusion of basolateral proteins. Ultimately the separation of two polarized membrane domains gives rise to the formation of a tight junction. Pals1, Patj, and Par3 staining is restricted to the tight junction and excludes the apical membrane domain.

plasmic accumulations, indicating a functional difference between VACs under low-calcium conditions and the recycling endosomes we found in these studies. More research will be required to compare the observed compartments.

Once recruited, aPKCζ might serve to further reinforce apical identity at the forming apical membrane domain. Previous work has shown that aPKC-dependent phosphorylation of the basolateral proteins Par1 and Lgl is sufficient to exclude them from aPKC-positive areas (Plant *et al.*, 2003; Hurov *et al.*, 2004; Suzuki *et al.*, 2004), whereas Par1-kinase is able to phosphorylate Par3, leading to a disassembly of the Par–aPKC complex and thus its exclusion from Par1-positive areas (Benton and St. Johnston, 2003; Hurd *et al.*, 2003a). This mutual exclusion of apical and basolateral proteins is thought to lead to the definition of two distinct apical and basolateral membrane domains. Figure 2D demonstrates this separation, as seen for GFP-Crb3a, representing the apical domain, and E-cadherin, representing the basolateral domain. On the border of the successfully separated membrane domains, a TJ is generated, fortifying the physical separation of both domains (Figure 2D, see ZO-1 staining; Shin *et al.*, 2006). In accordance with this model, inhibition of aPKCζ with myristoylated pseudosubstrate leads to the ectopic localization of apical and tight junction proteins, in extreme cases even to the formation of multiple lumina already at a two-cell stage (Figure 8). This might be a result of incomplete exclusion of basolateral proteins from the forming apical domain with the result of several smaller apical areas which are separated by remaining domains of basolateral identity.

No-Lumen and Multiple-Lumen Phenotypes in Cyst Formation

In this article we present evidence that Crb3a is required for the definition of apical membrane identity. Knockdown of Crb3 leads to the absence of apical membrane and thus to the absence of emerging lumina at the two-cell stage (no-lumen phenotype, Figure 7). This result is supported by the previous observation that knockdown of Crb3 leads to the absence of lumina at later stages of cyst development (Torkko *et al.*, 2008). Because one of our Crb3 hairpins showed a reduction of GP135 levels (Supplemental Figure S7A), we cannot rule out a role for GP135 in lumen formation. Meder *et al.* (2005) found a requirement of GP135 for lumen formation, although this result could not be reproduced by Cheng *et al.* (2005). Furthermore, the second hairpin we used did not cause a reduction of GP135, compared with the control cell line used, although reproducing the predominant no-lumen phenotype of the first hairpin (Supplemental Figure S7B). To resolve any doubt, we performed rescue experiments, clearly demonstrating that GFP-Crb3a could rescue lumen formation, thus proving its importance to the process (Figure 7).

The formation of the multiple-lumen phenotype may be more complex. A very recent article examined the delivery of aPKC in the division of single MDCK cells and presented a model in which down-regulation of Cdc42 resulted in a multiple-lumen phenotype (Jaffe *et al.*, 2008). In this model, apical membrane is delivered by the midzone microtubules, and Cdc42 knockdown-dependent deviation of the mitotic axis in later cell divisions would result in the ectopic delivery of apical membrane, resulting in additional ectopic lumina. We show that Crb3a-positive apical membrane gets endocytosed into apical recycling endosomes only during early cell divisions during MDCK cyst formation, whereas we failed to detect any internalized Crb3a at mature stages of cyst formation, where an apical surface is already present (Figure 2E). We conclude that Crb3a gets "trapped" at the apical surface by an as yet unidentified mechanism. Additionally, aPKCζ inhibition with myristoylated pseudosubstrate can result in a multiple-lumen phenotype already at the two-cell stage, without the possibility of ectopic membrane delivery caused by a disoriented mitotic axis in multiple cell divisions (Figure 8). Thus both mechanisms might work together in order to result in the observed multiple-lumen phenotype that has been reported in many publications (Straight *et al.*, 2004; Shin *et al.*, 2005; Jaffe *et al.*, 2008).

Taken together, we have provided evidence that a cell division of a single MDCK cell embedded into ECM can create a lumen dependent on the delivery of Crb3a-positive apical membrane in Rab11-positive endosomes during the course of cytokinesis (Figure 9). Further work will clarify open questions, such as how the initial uptake of Crb3a at the one-cell stage takes place and what molecular mechanisms underlie the docking and fusion of Crb3a-positive vesicles during the formation of the very first lumen.

ACKNOWLEDGMENTS

We thank Jennifer Harder-Krans for inspiring discussions, Dr. Stephen Lentz from the Morphology and Image of the Michigan Diabetes and Training Center, University of Michigan, and Dr. Chris Edwards from the Microscopy and Image Analysis Laboratory, University of Michigan, for their help and advice. This work was supported by National Institutes of Health (NIH) Grants DK058208 and DK069605 (B.M.), National Institute of Diabetes and Digestive and Kidney Diseases Grant NIH5P60 DK20572 (B.M.), Deutsche Forschungsgemeinschaft (DFG) Grant SCHL 1845/1-1 (M.S.), Medical Faculty of the University of Münster, Germany IMF Grant I-WE110719 to Medizinische Klinik D, NIH National Research Service Award GM079906 (E.L.W.), PKD Foundation Grant 162G08a and Fellowship 92a2f (T.H.).

REFERENCES

Benton, R., and St. Johnston, D. (2003). *Drosophila* PAR-1 and 14-3-3 inhibit Bazooka/PAR-3 to establish complementary cortical domains in polarized cells. Cell *115*, 691–704.

Bhartur, S. G., Calhoun, B. C., Woodrum, J., Kurkjian, J., Iyer, S., Lai, F., and Goldenring, J. R. (2000). Genomic structure of murine Rab11 family members. Biochem. Biophys. Res. Commun. *269*, 611–617.

Boutet, A., De Frutos, C. A., Maxwell, P. H., Mayol, M. J., Romero, J., and Nieto, M. A. (2006). Snail activation disrupts tissue homeostasis and induces fibrosis in the adult kidney. EMBO J. *25*, 5603–5613.

Cheng, H. Y., *et al.* (2005). Molecular identification of canine podocalyxin-like protein 1 as a renal tubulogenic regulator. J. Am. Soc. Nephrol. *16*, 1612–1622.

Cresawn, K. O., Potter, B. A., Oztan, A., Guerriero, C. J., Ihrke, G., Goldenring, J. R., Apodaca, G., and Weisz, O. A. (2007). Differential involvement of endocytic compartments in the biosynthetic traffic of apical proteins. EMBO J. *26*, 3737–3748.

Fan, S., Fogg, V., Wang, Q., Chen, X. W., Liu, C. J., and Margolis, B. (2007). A novel Crumbs3 isoform regulates cell division and ciliogenesis via importin beta interactions. J. Cell Biol. *178*, 387–398.

Ferrari, A., Veligodskiy, A., Berge, U., Lucas, M. S., and Kroschewski, R. (2008). ROCK-mediated contractility, tight junctions and channels contribute to the conversion of a preapical patch into apical surface during isochoric lumen initiation. J. Cell Sci. *121*, 3649–3663.

Fogg, V. C., Liu, C. J., and Margolis, B. (2005). Multiple regions of Crumbs3 are required for tight junction formation in MCF10A cells. J. Cell Sci. *118*, 2859–2869.

Hobdy-Henderson, K. C., Hales, C. M., Lapierre, L. A., Cheney, R. E., and Goldenring, J. R. (2003). Dynamics of the apical plasma membrane recycling system during cell division. Traffic *4*, 681–693.

Horgan, C. P., Walsh, M., Zurawski, T. H., and McCaffrey, M. W. (2004). Rab11-FIP3 localises to a Rab11-positive pericentrosomal compartment during interphase and to the cleavage furrow during cytokinesis. Biochem. Biophys. Res. Commun. *319*, 83–94.

Horikoshi, Y., Suzuki, A., Yamanaka, T., Sasaki, K., Mizuno, K., Sawada, H., Yonemura, S., and Ohno, S. (2009). Interaction between PAR-3 and the aPKC-PAR-6 complex is indispensable for apical domain development of epithelial cells. J. Cell Sci. *122*, 1595–1606.

Hurd, T. W., Fan, S., Liu, C. J., Kweon, H. K., Hakansson, K., and Margolis, B. (2003a). Phosphorylation-dependent binding of 14-3-3 to the polarity protein Par3 regulates cell polarity in mammalian epithelia. Curr. Biol. *13*, 2082–2090.

Hurd, T. W., Gao, L., Roh, M. H., Macara, I. G., and Margolis, B. (2003b). Direct interaction of two polarity complexes implicated in epithelial tight junction assembly. Nat. Cell Biol *5*, 137–142.

Hurov, J. B., Watkins, J. L., and Piwnica-Worms, H. (2004). Atypical PKC phosphorylates PAR-1 kinases to regulate localization and activity. Curr. Biol. *14*, 736–741.

Ikenouchi, J., Matsuda, M., Furuse, M., and Tsukita, S. (2003). Regulation of tight junctions during the epithelium-mesenchyme transition: direct repression of the gene expression of claudins/occludin by Snail. J. Cell Sci. *116*, 1959–1967.

Jaffe, A. B., Kaji, N., Durgan, J., and Hall, A. (2008). Cdc42 controls spindle orientation to position the apical surface during epithelial morphogenesis. J. Cell Biol. *183*, 625–633.

Lemmers, C., Medina, E., Lane-Guermonprez, L., Arsanto, J. P., and Le Bivic, A. (2004a). [Role of Crumbs proteins in the control of epithelial cell and photoreceptor morphogenesis]. Med. Sci. (Paris) *20*, 663–667.

Lemmers, C., Michel, D., Lane-Guermonprez, L., Delgrossi, M. H., Medina, E., Arsanto, J. P., and Le Bivic, A. (2004b). CRB3 binds directly to Par6 and regulates the morphogenesis of the tight junctions in mammalian epithelial cells. Mol. Biol. Cell *15*, 1324–1333.

Lubarsky, B., and Krasnow, M. A. (2003). Tube morphogenesis: making and shaping biological tubes. Cell *112*, 19–28.

Makarova, O., Roh, M. H., Liu, C. J., Laurinec, S., and Margolis, B. (2003). Mammalian Crumbs3 is a small transmembrane protein linked to protein associated with Lin-7 (Pals1). Gene *302*, 21–29.

Martin-Belmonte, F., Gassama, A., Datta, A., Yu, W., Rescher, U., Gerke, V., and Mostov, K. (2007). PTEN-mediated apical segregation of phosphoinositides controls epithelial morphogenesis through Cdc42. Cell *128*, 383–397.

Martin-Belmonte, F., and Mostov, K. (2008). Regulation of cell polarity during epithelial morphogenesis. Curr. Opin. Cell Biol. *20*, 227–234.

Martin-Belmonte, F., Yu, W., Rodriguez-Fraticelli, A. E., Ewald, A., Werb, Z., Alonso, M. A., and Mostov, K. (2008). Cell-polarity dynamics controls the mechanism of lumen formation in epithelial morphogenesis. Curr. Biol. *18*, 507–513.

Martinez-Estrada, O. M., Culleres, A., Soriano, F. X., Peinado, H., Bolos, V., Martinez, F. O., Reina, M., Cano, A., Fabre, M., and Vilaro, S. (2006). The transcription factors Slug and Snail act as repressors of Claudin-1 expression in epithelial cells. Biochem. J. *394*, 449–457.

Meder, D., Shevchenko, A., Simons, K., and Fullekrug, J. (2005). Gp135/podocalyxin and NHERF-2 participate in the formation of a preapical domain during polarization of MDCK cells. J. Cell Biol. *168*, 303–313.

Nokes, R. L., Fields, I. C., Collins, R. N., and Folsch, H. (2008). Rab13 regulates membrane trafficking between TGN and recycling endosomes in polarized epithelial cells. J. Cell Biol. *182*, 845–853.

O'Brien, L. E., Zegers, M. M., and Mostov, K. E. (2002). Opinion: Building epithelial architecture: insights from three-dimensional culture models. Nat. Rev. Mol. Cell Biol. *3*, 531–537.

Omori, Y., and Malicki, J. (2006). oko meduzy and related crumbs genes are determinants of apical cell features in the vertebrate embryo. Curr. Biol. *16*, 945–957.

Plant, P. J., Fawcett, J. P., Lin, D. C., Holdorf, A. D., Binns, K., Kulkarni, S., and Pawson, T. (2003). A polarity complex of mPar-6 and atypical PKC binds, phosphorylates and regulates mammalian Lgl. Nat. Cell Biol. *5*, 301–308.

Roh, M. H., Fan, S., Liu, C. J., and Margolis, B. (2003). The Crumbs3-Pals1 complex participates in the establishment of polarity in mammalian epithelial cells. J. Cell Sci. *116*, 2895–2906.

Roh, M. H., Makarova, O., Liu, C. J., Shin, K., Lee, S., Laurinec, S., Goyal, M., Wiggins, R., and Margolis, B. (2002). The Maguk protein, Pals1, functions as an adapter, linking mammalian homologues of Crumbs and Discs Lost. J. Cell Biol. *157*, 161–172.

Sato, T., *et al*. (2007). The Rab8 GTPase regulates apical protein localization in intestinal cells. Nature *448*, 366–369.

Saxen, L. (1987). Organogenesis of The Kidney, Cambridge: Cambridge University Press.

Schlüter, M. A., and Margolis, B. (2009). Apical lumen formation in renal epithelia. J. Am. Soc. Nephrol. *20*, 1444–1452.

Shin, K., Fogg, V. C., and Margolis, B. (2006). Tight junctions and cell polarity. Annu. Rev. Cell Dev. Biol. *22*, 207–235.

Shin, K., Straight, S., and Margolis, B. (2005). PATJ regulates tight junction formation and polarity in mammalian epithelial cells. J. Cell Biol. *168*, 705–711.

Straight, S. W., Shin, K., Fogg, V. C., Fan, S., Liu, C. J., Roh, M., and Margolis, B. (2004). Loss of PALS1 expression leads to tight junction and polarity defects. Mol. Biol. Cell *15*, 1981–1990.

Suzuki, A., *et al*. (2004). aPKC acts upstream of PAR-1b in both the establishment and maintenance of mammalian epithelial polarity. Curr. Biol. *14*, 1425–1435.

Tawk, M., Araya, C., Lyons, D. A., Reugels, A. M., Girdler, G. C., Bayley, P. R., Hyde, D. R., Tada, M., and Clarke, J. D. (2007). A mirror-symmetric cell division that orchestrates neuroepithelial morphogenesis. Nature *446*, 797–800.

Thiery, J. P., and Sleeman, J. P. (2006). Complex networks orchestrate epithelial-mesenchymal transitions. Nat. Rev. Mol. Cell Biol. *7*, 131–142.

Torkko, J. M., Manninen, A., Schuck, S., and Simons, K. (2008). Depletion of apical transport proteins perturbs epithelial cyst formation and ciliogenesis. J. Cell Sci. *121*, 1193–1203.

van Ijzendoorn, S. C. (2006). Recycling endosomes. J. Cell Sci. *119*, 1679–1681.

Vega-Salas, D. E., Salas, P. J., and Rodriguez-Boulan, E. (1987). Modulation of the expression of an apical plasma membrane protein of Madin-Darby canine kidney epithelial cells: cell-cell interactions control the appearance of a novel intracellular storage compartment. J. Cell Biol. *104*, 1249–1259.

Wang, Q., and Margolis, B. (2007). Apical junctional complexes and cell polarity. Kidney Int. *72*, 1448–1458.

Wang, X., Kumar, R., Navarre, J., Casanova, J. E., and Goldenring, J. R. (2000). Regulation of vesicle trafficking in madin-darby canine kidney cells by Rab11a and Rab25. J. Biol. Chem. *275*, 29138–29146.

Whiteman, E. L., Liu, C. J., Fearon, E. R., and Margolis, B. (2008). The transcription factor snail represses Crumbs3 expression and disrupts apico-basal polarity complexes. Oncogene *27*, 3875–3879.

Wodarz, A., Hinz, U., Engelbert, M., and Knust, E. (1995). Expression of crumbs confers apical character on plasma membrane domains of ectodermal epithelia of *Drosophila*. Cell *82*, 67–76.